Effects of approximation of self-excited forces by rational function on wind-induced response of a long-span bridge

Nguyen Danh Thang [*], Hiroshi Katsuchi [**], Hitoshi Yamada [***] and Eiichi Sasaki [**]

* M. of Eng., Dept. of Civil Eng., Yokohama National University, Yokohama 240-8501
**Dr. of Eng., Assoc. Prof., Dept. of Civil Eng., Yokohama National University, Yokohama 240-8501
*** Dr. of Eng., Prof., Dept. of Civil Eng., Yokohama National University, Yokohama 240-8501

In this paper, time-domain modeling of bridge deck flutter is first developed. The frequency dependent self-excited forces acting on a bridge deck are approximated in the Laplace transform domain by rational functions. The least-square matrix formulation of the rational function approximation is applied to flutter derivatives of the Akashi Kaikyo Bridge and airfoil. Besides, numerical analyses of the wind-induced response of the Akashi Kaikyo Bridge were conducted to facilitate the discussion. After that, the vertical deflection and torsion at the span center of the Akashi Kaikyo Bridge caused by buffeting and self-excited forces using the results of approximated flutter derivatives are examined to investigate the sensitivity of the approximation to the wind-induced response.

Key Words: rational function approximation, self-excited force, time-domain analysis

1. Introduction

Long-span cable supported bridges are inherently lightly damped and flexible. Therefore, these bridges are susceptible to wind induced instabilities. Flutter and galloping are destructive phenomena and need special attention. Safety against flutter may be ensured by keeping the critical wind speed well above the design wind speed at the bridge site.

Self-excited forces causing flutter are in general dependent on the geometric profile of the bridge deck section, angle of wind attack and wind velocity expressed as reduced frequency. Scanlan[1)] expressed self-excited lift, drag and pitching moment in terms of flutter derivatives and associated structural motions. The analytical approach adopted by Scanlan[1)], Scanlan and Jones[2)], Jain et al[3)] is predominantly in frequency domain. However, the frequency domain approach is restricted to linear structures excited by stationary winds without aerodynamic nonlinearities such as the sudden change of mean wind speed and transient response at near the flutter critical wind speed. Recently, an analytical procedure in time domain has been proposed by Boonyapinyo et al[4)] and Chen et al[5)] by the introduction of rational function approximation of self-excited forces.

In the past, frequency domain analysis dominated due to the efficiency of computation, especially when handling the unsteady aeroelastic forces that are functions of reduced frequency. The nature of flutter analysis is generally a complex eigenvalue problem. With increasing the length of bridge span, the structure becomes more flexible. It's necessary to transform the analytical method from frequency domain into time domain to overcome the difficulties in dealing with those nonlinearities.

Recently, an efficient scheme for a coupled multimode flutter analysis has been proposed introducing the unsteady self-exited aerodynamic forces in terms of the rational function approximations[4), 5)]. This has led to a convenient transformation of the equation into a state space format independent of reduced frequency. A significant feature of this approach is that an iterative solution for determining flutter boundary is unnecessary because the equations are independent of the reduced frequency $K = \omega B / U$ where ω is the circular frequency, B is the deck width and U is the wind velocity. To include those nonlinearities of structural and aerodynamic origins, the time domain approach is more appropriate. Time domain approach, however, involves the transformation of flutter derivatives into indicial functions, which have inherent deficit. The effectiveness of the time domain analysis in calculating buffeting response depends on the establishment of an effective time domain model for the self-excited wind force. However, few studies on accuracy of the approximation were made.

In this study, sensitivity of approximation accuracy in the rational function approximation for self-excited forces is investigated with respect to the approximation error and wind-induced response with the approximation result. Some guidelines for wind-induced response analysis in time domain with the rational function approximation method will be clarified.

2. Equation of Motion of Bridge Deck

A basic task in the study of the bridge aeroelasticity is to formulate the wind forces on the structure. Considering a section of bridge deck subjected to the action of a smooth oncoming flow, the section is assumed to have two degrees of freedom: heaving displacement h and rotation α as shown in Fig. 1. A unit sectional model has mass m, polar moment of inertia I, coefficient of viscous damping C_h and C_α, and vertical and stiffness coefficients of the heaving and pitching modes K_h and K_α. With these definitions, the equations of motion of a bridge deck can be written as follows:

$$m\ddot{h} + C_h\dot{h} + K_h h = L \tag{1a}$$

$$I\ddot{\alpha} + C_\alpha\dot{\alpha} + K_\alpha\alpha = M \tag{1b}$$

where L and M are the lift and pitching moment about the rotation axis per unit span length, respectively. The lift and pitching moment per unit span can be defined by:

Lift: $$L = L_{ae} + L_b \tag{2a}$$

Pitching moment: $$M = M_{ae} + M_b \tag{2b}$$

where the subscripts ae and b refer to aeroelastic and buffeting, respectively.

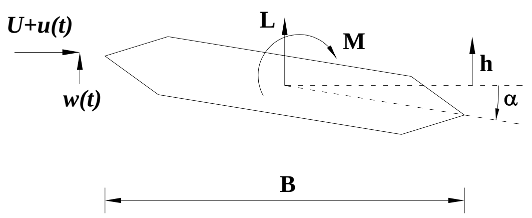

Fig.1 Two degrees of freedom model of bridge deck

Special considerations are needed for the formulation of self-excited forces for a bridge deck. The signature turbulence, in the case of an efficient airfoil in a smooth flow, is intentionally reduced by careful streamlining with notable attention to the introduction of a sharp trailing edge. For bluff bodies, however, the situation is different. The use of Theodorsen aerodynamics for such bluff bodies is not guaranteed correct. In view of this, the formulation of self-exited forces on civil engineering structures, such as a bridge deck, is more experimental than theoretical. Scanlan[1)] suggested the reduced frequency dependent flutter derivatives could be used in the modeling of self-excited forces on a bridge deck. This is the counterpart of the Theodorsen theory in the experimental bridge aerodynamics. The flutter derivative format representation of self-excited forces takes the form for two degrees of freedom:

$$L_{ae} = \frac{1}{2}\rho U^2 B\left[KH_1^*\frac{\dot{h}}{U} + KH_2^*\frac{B\dot{\alpha}}{U} + K^2H_3^*\alpha + K^2H_4^*\frac{h}{B}\right] \tag{3a}$$

$$M_{ae} = \frac{1}{2}\rho U^2 B^2\left[KA_1^*\frac{\dot{h}}{U} + KA_2^*\frac{B\dot{\alpha}}{U} + K^2A_3^*\alpha + K^2A_4^*\frac{h}{B}\right] \tag{3b}$$

where ρ is the air density; U is the mean wind velocity; B is the width of the section model; $K = B\omega/U$ is the reduced frequency, ω is the circular frequency of oscillation; and the non-dimensional aerodynamic coefficient H_i^* and A_i^* (i = 1, 2, 3, 4) are the flutter derivatives of a cross section as a function of the reduced frequency.

Under assumed relatively slowly varying gust action, the buffeting forces are defined as:

$$L_b = \frac{1}{2}\rho U^2 B\left[C_L\left(2\frac{u}{U}\right) + C_L'\frac{w}{U}\right] \tag{4a}$$

$$M_b = \frac{1}{2}\rho U^2 B^2\left[C_M\left(2\frac{u}{U}\right) + C_M'\frac{w}{U}\right] \tag{4b}$$

where C_L and C_M are the static lift and pitching moment coefficients (referred to deck width B) of a typical deck station, respectively; $C_L' = dC_L/d\alpha$ and $C_M' = dC_M/d\alpha$; and $u = u(t)$ and $w = w(t)$ are the along-wind and vertical velocity fluctuations of the wind, respectively.

3. Rational Function Approximation of Aeroelastic Forces

To analyze aeroelastic forces, frequency-dependent aeroelastic forces are often transformed into time-dependent forces so that they can be applied in the explicit time-domain approach. The most common form of the approximation function for aeroelastic force coefficients is a rational function of the non-dimensional Laplace variable p (non-dimensional Laplace variable, $p = sB/U = iK$, where non-dimensional time $s = Ut/B$ and unit imaginary number $i = \sqrt{-1}$). For the two degrees of freedom section model, the equations of motion, considering aeroelastic forces only, can be written in the Laplace transform domain (L denotes the Laplace operator) with zero initial condition as:

$$\begin{aligned}&(\underline{M}p^2(U/B)^2 + \underline{C}p(U/B) + \underline{K})L(\underline{q}) \\ &= \underline{V}_f\underline{\tilde{Q}}L(\underline{q}) = \underline{V}_f\underline{\tilde{Q}}\underline{\hat{q}}\end{aligned} \tag{5}$$

Coefficient matrices in equation (5) are defines as:

$$\underline{M} = \begin{bmatrix} mB & 0 \\ 0 & I \end{bmatrix}, \quad \underline{C} = \begin{bmatrix} C_hB & 0 \\ 0 & C_\alpha \end{bmatrix},$$

$$\underline{K} = \begin{bmatrix} K_hB & 0 \\ 0 & K_\alpha \end{bmatrix}, \quad \underline{q} = \begin{bmatrix} h/B \\ \alpha \end{bmatrix},$$

$$\underline{V}_f = \begin{bmatrix} -0.5\rho U^2 B & 0 \\ 0 & 0.5\rho U^2 B^2 \end{bmatrix},$$

$$\underline{\tilde{Q}} = \begin{bmatrix} K_n^2 H_4^* + pK_n H_1^* & K_n^2 H_3^* + pK_n H_2^* \\ K_n^2 A_4^* + pK_n A_1^* & K_n^2 A_3^* + pK_n A_2^* \end{bmatrix}$$

$$= \begin{bmatrix} K_n^2 H_4^* + iK_n^2 H_1^* & K_n^2 H_3^* + iK_n^2 H_2^* \\ K_n^2 A_4^* + iK_n^2 A_1^* & K_n^2 A_3^* + iK_n^2 A_2^* \end{bmatrix}$$

Each component of matrix $\underline{\tilde{Q}}$ in equation (5) is complex number including two parts: real part ($K_n^2 X_i^*$, $X_i^* = H_4^*, H_3^*, A_4^*, A_3^*$) and imaginary part ($K_n^2 X_j^*$, $X_j^* = H_1^*, H_2^*, A_1^*, A_2^*$). K_n is the n-th reduced frequency in measurement.

Thus, aeroelastic lift and pitching moment per unit span length of the section model expressed in the Laplace transform domain can be written as follows:

$$\begin{Bmatrix} \hat{L}_{ae} \\ \hat{M}_{ae} \end{Bmatrix} = \underline{V}_f \underline{\tilde{Q}} \underline{\hat{q}}$$
$$= \begin{bmatrix} -0.5\rho U^2 B & 0 \\ 0 & 0.5\rho U^2 B \end{bmatrix} \begin{bmatrix} K_n^2 H_4^* + iK_n^2 H_1^* & K_n^2 H_3^* + iK_n^2 H_2^* \\ K_n^2 A_4^* + iK_n^2 A_1^* & K_n^2 A_3^* + iK_n^2 A_2^* \end{bmatrix} \begin{Bmatrix} \hat{h}/B \\ \hat{\alpha} \end{Bmatrix} \tag{6}$$

where '^' denotes the transformation in the Laplace domain.

Approximation of the aeroelastic forces as the rational function of a Laplace variable allows the equations of motion to be written in a linear time invariant state-space realization. There are several variations of the matrix form of the rational function approximation for unsteady aeroelastic force coefficients. Two major variations are the least-squares formulation and minimum state formulation. Each matrix formulation results in a different aerodynamic state vector. In this study, the least-square method was used to approximate the aeroelastic forces.

Roger[7] formulated the rational function approximation using the least-square method as follows:

$$\hat{\mathbf{Q}}(iK) = \mathbf{A}_0 + (iK)\mathbf{A}_1 + \sum_{l=1}^{n_l} \frac{1}{iK + \lambda_l} \mathbf{A}_{l+1} \tag{7}$$

Each matrix in equation (7) is a square matrix, with the dimension $n \times n$ (n is number of degrees of freedom of the section model). The element of A_0, A_1 represent aerodynamic stiffness and damping, respectively. The partial fractions, $A_{l+1}/(iK + \lambda_l)$, are commonly called "lag terms" as each represents a transfer function in which output "lag" behind the input and approximates the inherent time delays associated with unsteady aerodynamic forces. The coefficients of the partial fractions λ_l are referred as "lag coefficients". Because the 3rd clause of equation (7) has the shape of the rational function, this approximation method is called a rational function approximation technique.

To minimize the error of approximation process, we can increase the number of lag terms. However, this action also means we have to increase the number of required equations to define the aerodynamic system. Improvement can also be realized by decreasing the frequency range over which the fits are required, but this narrows the applicability of the approximation. The additional improvements may be obtained by an optimization of the lag coefficients.

Each component of $\hat{Q}(iK)$ can be written as

$$\begin{aligned} \hat{Q}_{ij}(iK) &= (A_0)_{ij} + (A_1)_{ij} iK + \sum_{\ell=1}^{n\ell} (A_{\ell+1})_{ij} \frac{1}{iK + \lambda_\ell} \\ &= \left[(A_0)_{ij} + \sum_{\ell=1}^{n\ell} (A_{\ell+1})_{ij} \frac{\lambda_\ell}{K^2 + \lambda_\ell{}^2} \right] \\ &\quad + i \left[(A_1)_{ij} K - \sum_{\ell=1}^{n\ell} (A_{\ell+1})_{ij} \frac{K}{K^2 + \lambda_\ell{}^2} \right] \end{aligned} \tag{8}$$

where the reduced frequency K is defined as

$$K = \frac{B\omega}{U} = \frac{B(2\pi n)}{U} \tag{9}$$

From equation (9), it is easily seen that the coefficients $(A_0)_{ij}$, $(A_1)_{ij}$, and $(A_{l+1})_{ij}$ may be found through a linear optimization but the lag coefficients must be found by using a nonlinear optimization method. Determination of parameters of approximation functions is divided into two parts: optimization of coefficients $(A_m)_{ij}$ ($i, j = 1, \ldots, n$; $m = 0, \ldots, n_l + 1$) and search for λ_l.

To define the linear parameters in the rational function approximation, the error function between the approximate data and the actual tabular data for each aerodynamic force element is defined as follows:

$$\varepsilon_{ij} = \frac{\sum_n \left\| \hat{Q}_{ij}(iK_n) - Q_{ij}(iK_n) \right\|^2}{M_{ij}} \tag{10}$$

where $\hat{Q}_{ij}$ and Q_{ij} are the approximation and tabular value of matrix Q, respectively; $\mathrm{Re}(Q_{ij}(iK_n))$ and $\mathrm{Im}(Q_{ij}(iK_n))$ are the real part and imaginary part of Q, respectively; $\{K_n\}$ is a set of reduced frequencies for which tabular data are available, and

$$M_{ij} = \max\left\{1, \left\| Q_{ij}(ik_n) \right\|^2 \right\} \tag{11}$$

To evaluate the error margin of each element of $Q(iK_n)$ as evenly as possible, the second part of the error margin is added with M_{ij} of expression (11). Each term in the sum in equation (11) is a measure of relative error if the maximum magnitude of $Q_{ij}(iK_n)$ is larger than 1, but it becomes an absolute error for magnitudes smaller than 1. This error function essentially normalizes the aerodynamic data prior to the nonlinear optimization.

To minimize the value of ε_{ij} when considering the function of $\boldsymbol{A}_{nl+1}$, $(A_m)_{ij}$ should fill the following relation.

$$\frac{\partial \varepsilon_{ij}}{\partial (A_m)_{ij}} = 0 \qquad (for \quad m = 0, \cdots, n_l + 1) \tag{12}$$

To determine the nonlinear parameters in the rational function approximation, the nongradient method was developed[6]. In this application, the nongradient optimizer was also confirmed to be numerically stable and to possess good convergence properties. The evaluation function J will be used to reduce the total approximation errors, $J = \sqrt{\sum_{i=1}^{2}\sum_{j=1}^{2} w_{ij}\varepsilon_{ij}}$. The weighting factors w_{ij} are used to force some of the elements to have more priority than others in determining the lag coefficients.

The process of approximation for both linear and nonlinear is shown in Fig. 2 in which the value A_{ij} and λ_{ij} can be defined so as to minimize the value of the evaluation function J. After that, the approximation results of Q_{ij} are obtained.

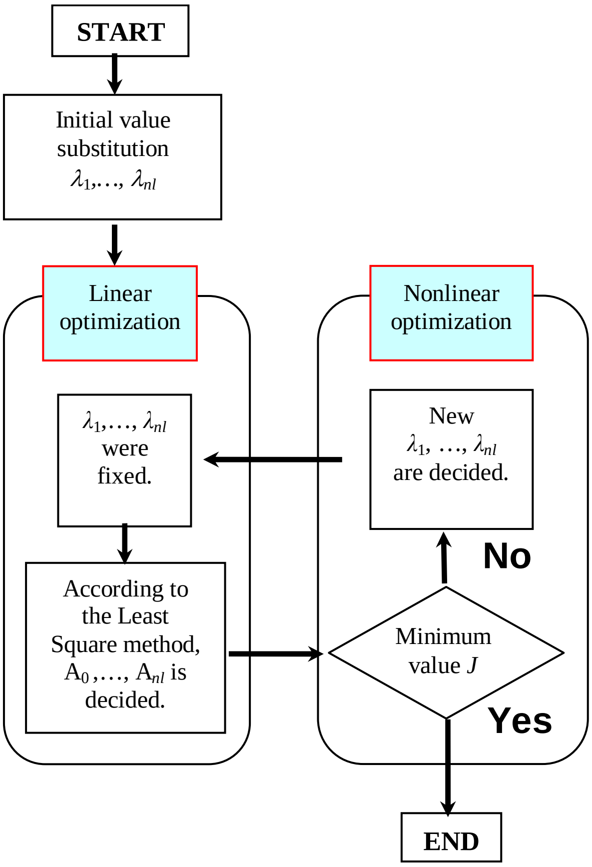

Fig. 2 Flow chart of rational function approximation process

4. Application of Rational Function Approximation

In this study, both Theodorsen theory and Akashi Kaikyo Bridge data were used to compare the results between approximation and tabular data.

4.1 Theodorsen Theory

In Theodorsen theory, when the oscillation is sinusoidal, the flutter derivatives for a bridge deck can be defined as follows[1]:

$$K^2H_1^* = -2\pi KF \tag{13a}$$

$$K^2H_2^* = \frac{-\pi K}{2}\left[1+\frac{4G}{K}+F\right] \tag{13b}$$

$$K^2H_3^* = -\pi\left[2F-\frac{GK}{2}\right] \tag{13c}$$

$$K^2H_4^* = \frac{\pi}{2}K^2\left[1+\frac{4G}{K}\right] \tag{13d}$$

$$K^2A_1^* = \frac{\pi}{2}KF \tag{13e}$$

$$K^2A_2^* = \frac{-\pi}{2}\left[\frac{K}{4}-G-\frac{KF}{4}\right] \tag{13f}$$

$$K^2A_2^* = \frac{-\pi}{2}\left[\frac{K}{4}-G-\frac{KF}{4}\right] \tag{13g}$$

$$K^2A_3^* = \frac{\pi}{2}\left[\frac{K^2}{32}+F-\frac{KG}{4}\right] \tag{13h}$$

$$K^2A_4^* = \frac{-\pi}{2}KG \tag{13i}$$

where the functions F and G are the real and imaginary part of Theodorsen's circulation function.

Fig. 3 shows the approximation results $\hat{Q}_{ij}$ of Theodorsen flutter derivatives with 2 and 3 lag terms in case the weight factor $w_{ij}=1$ is used. For Theodorsen theory, the approximation results are not so different in case more than 3 lag terms are used. The total errors for Theodorsen theory with more lag terms will be presented later in Fig. 5.

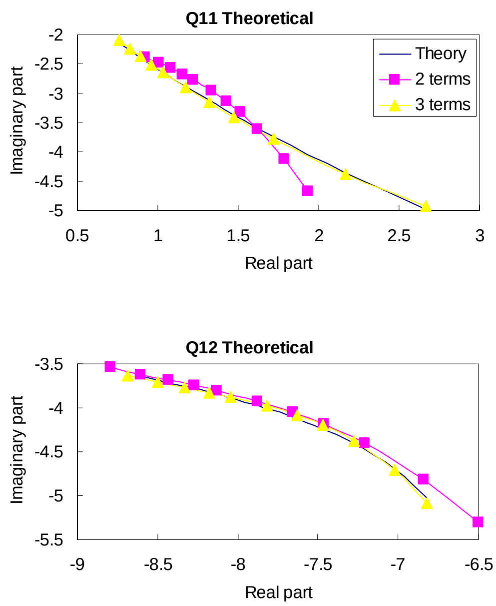

Fig. 3 Approximation results using 2 and 3 lag terms for Theodorsen theory

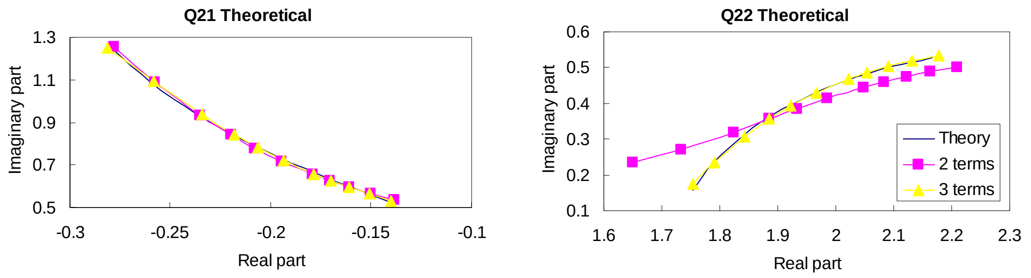

Fig. 3 Approximation results using 2 and 3 lag terms for Theodorsen theory (cont.)

4.2 Akashi Kaikyo Bridge

In this part, the results of the Akashi Kaikyo Bridge wind tunnel test with two cross sections (original section and modified section) will be used to analyze by using the rational function approximation technique. With each section, the tabular data for other angles of attack are also considered to compare the approximate results. The obtained results for the original section with 0 degree of angle of attack (α_a) are shown in Fig. 4. For the Akashi Kaikyo Bridge, the approximated result of component Q_{22} in most cases is not so good although 6 or 7 lag terms were used. However, the approximation results are almost same after 5 terms.

Fig. 5 shows the total errors between approximate result and Theodorsen theory or tabular data of the Akashi Kaikyo Bridge in other cases, using the weighting factor w_{ij} = 1. For most cases, the total error will decrease very fast from 2 lag terms to 4 lag terms, and after 5 lag terms the total error is almost constant. The slow decrease of the total error in the modified cross section of -3 degree may be due to point deviation of measurement value of a flutter derivative.

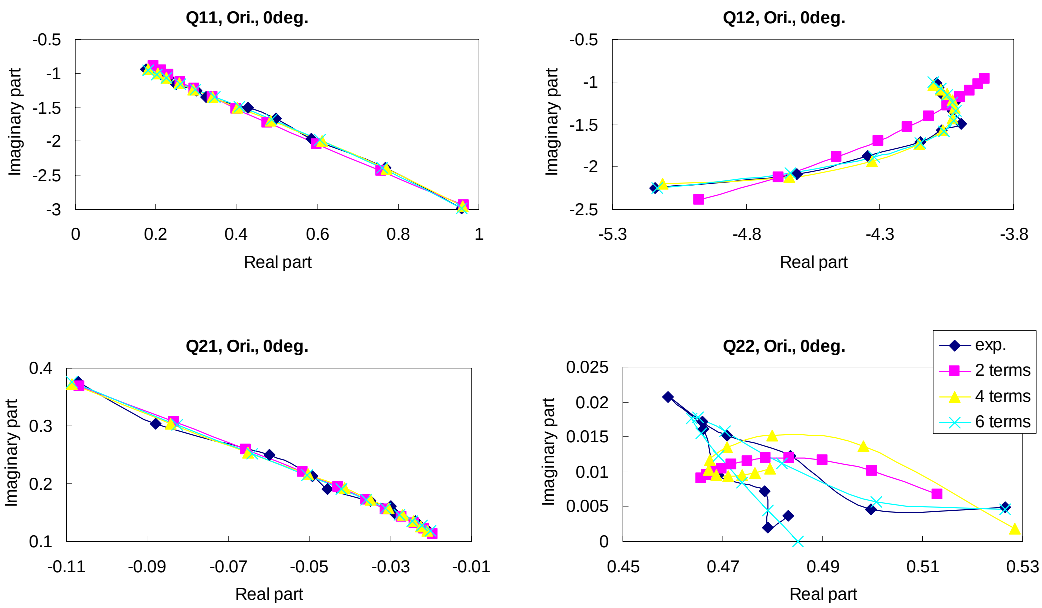

Fig. 4 Approximation results using 2, 4 and 6 lag terms for original section, α_a = 0 degree

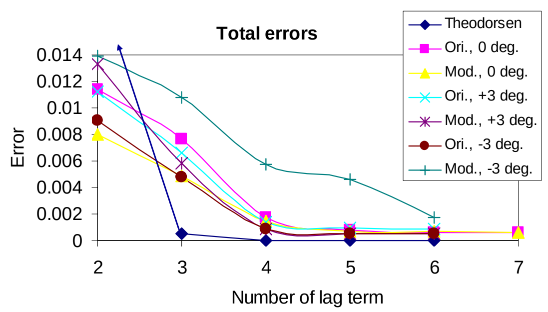

Fig. 5 Total error between approximation result and experiment result

5. Structure's Response Analysis

For the Akashi Kaikyo Bridge, the power spectral densities of along-wind and vertical velocity fluctuations of the wind were modeled using the Hino spectrum and Busch & Panofsky spectrum, respectively, based on the measurements in the wind tunnel. Turbulence intensities I_u = 0.1, I_w = 0.05 for turbulent components $u(t)$ and $w(t)$, respectively, are used to generate wind speed. Fig. 6 shows an example time history of along-wind and vertical velocity fluctuation of the wind speed of 60 m/s.

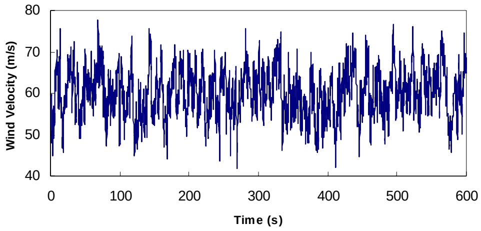

a) Along-wind velocity fluctuation

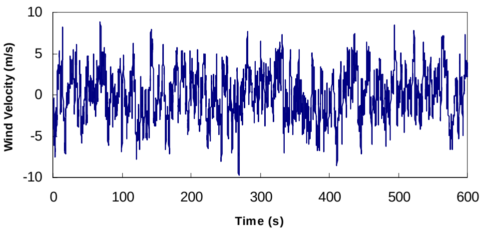

b) Vertical component of wind fluctuation

Fig. 6 Time history of wind speed fluctuation (U = 60 m/s)

In this study, the response at the span center of the Akashi Kaikyo Bridge, during 600 seconds, was analyzed at a set of mean wind velocity from 20 m/s to 110 m/s in two cases: first case is buffeting force only applied and second case is both buffeting and self-excited forces applied. The analysis was done with fundamental two modes: 1st symmetric vertical mode (f_1 = 0.065Hz) and 1st symmetric torsional mode (f_2 = 0.15Hz). Other structural and aerostatic parameters are $m = 44.0 \times 10^3$ kg, $I = 1.0 \times 10^7$ kgm^2, ζ_h= 0.03/2π, ζ_α= 0.02/2π, C_L = 0.1, C_L' = 1.9, C_M = 0.01 and C_M' = 0.27.

In the case of both buffeting and self-excited forces applied, the equation of motion of two degrees of freedom bridge deck model can be approximately expressed as[8)]

$$M\ddot{X} + C_{ef}\dot{X} + K_{ef}X = Q_b \qquad (14)$$

where

$$M = \begin{bmatrix} m & 0 \\ 0 & I \end{bmatrix}$$

$$C_{ef} = \begin{bmatrix} 2m\xi_h\omega_h - \rho\omega_1 b^2 H_1^*(k_1) & -\rho\omega_2 b^3 H_2^*(k_2) \\ -\rho\omega_1 b^3 A_1^*(k_1) & 2I\xi_\alpha\omega_\alpha - \rho\omega_2 b^4 A_2^*(k_2) \end{bmatrix}$$

$$K_{ef} = \begin{bmatrix} m\omega_h^2 - \rho\omega_1^2 b^2 H_4^*(k_1) & -\rho\omega_2^2 b^3 H_3^*(k_2) \\ -\rho\omega_1^2 b^3 A_4^*(k_1) & I\omega_\alpha^2 - \rho\omega_2^2 b^4 A_3^*(k_2) \end{bmatrix}$$

$$X = \begin{bmatrix} h \\ \alpha \end{bmatrix}, \qquad Q_b = \begin{bmatrix} \frac{1}{2}\rho U^2 B\left[C_L\left(2\frac{u}{U}\right) + C_L'\frac{w}{U}\right] \\ \frac{1}{2}\rho U^2 B^2\left[C_M\left(2\frac{u}{U}\right) + C_M'\frac{w}{U}\right] \end{bmatrix}$$

m is mass; I is polar moment of inertia of bridge deck; $B = 2b$ is bridge deck width; ω_h, ω_α are natural circular frequencies in the vertical and torsional direction, respectively; ξ_h, ξ_α are damping ratios in the vertical and torsional direction; $k_1 = \omega_1 b/U$, $k_2 = \omega_2 b/U$ are reduced frequencies corresponding to the two modes; H_i^* and A_i^* (i = 1, 2, 3, 4) are flutter derivatives, which are functions of reduced frequency and approximated by the rational function approximation; C_{ef}, K_{ef} are effective aeroelastic stiffness and damping matrices.

By solving the equation of motion, the Newmark β method with $\Delta t = 0.2$ (s) was used and the response at the span center of the Akashi Kaikyo Bridge was obtained.

5.1 Theodorsen Theory

The response of the Akashi Kaikyo Bridge using the theoretical flutter derivatives was first analyzed. Figs. 7 and 8 show the vertical deflection and torsion at span center of the original section at wind speeds of 30 m/s and 40 m/s. With Theordorsen theory, at 30 m/s, there is no apparent divergence trend. However, the divergence phenomenon is going to occur at 40 m/s (Fig. 8b). Besides, the structure response, both vertical deflection and torsion, is not different between 2 lag terms and 3 lag terms. It can be said that the response is insensitive to the approximation error as shown in Fig. 3.

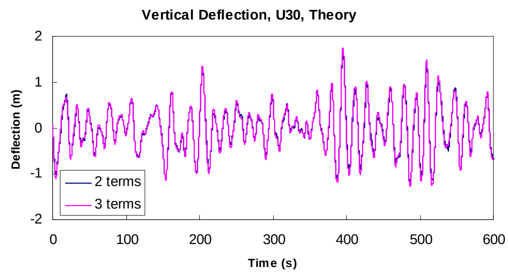

a) Vertical displacement, with 2and 3 lag terms

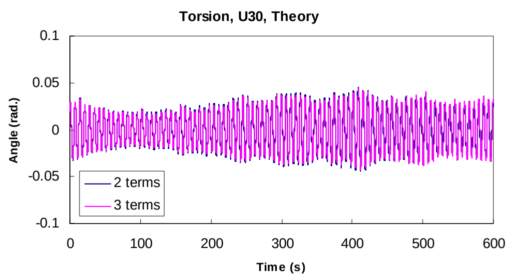

b) Torsion with 2 and 3 lag terms

Fig. 7 Responses of original section of Akashi Kaikyo Bridge with Theodorsen theory by buffeting and self-excited forces (U = 30 m/s)

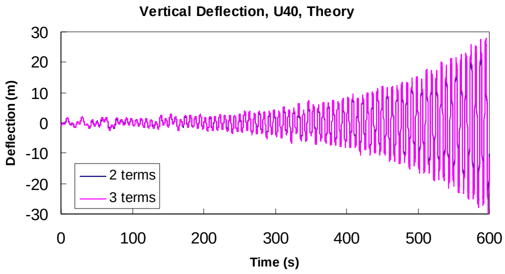

a) Vertical displacement with 2 and 3 lag terms

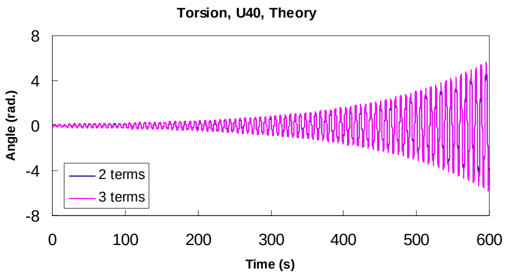

b) Torsion with 2 and 3 lag terms

Fig. 8 Responses of original section of Akashi Kaikyo Bridge with Theodorsen theory by buffeting and self-excited forces (U = 40 m/s)

5.2 Akashi Kaikyo (Original section, α_a = 0 degree)

For the Akashi Kaikyo Bridge, vertical deflection and torsion at 60 m/s with buffeting forces only applied is presented in Fig. 9. Quite large response in vertical was obtained. On the other hand, in the case of both buffeting and self-excited forces applied at 50 m/s, vertical response is decreased due to aerodynamic damping and torsional response shows a litter sinusoidal excitation due to self-excited force, as shown in Fig. 10. At this wind velocity of 50 m/s, no apparent divergence trend can be observed, but the torsional response shows more sinusoidal excitation and is going to diverge slowly at 60 m/s as shown in Fig. 11.

Similar to the result of Theodorsen theory in Section 5.1, although the approximate error is very different, the response of the bridge is almost same between 2 lag terms and 5 lag terms as shown in Figs. 10 and 11. This means the response is insensitive to approximate error within the error in this study. However, appropriateness of the convergence criteria should also be examined more specifically.

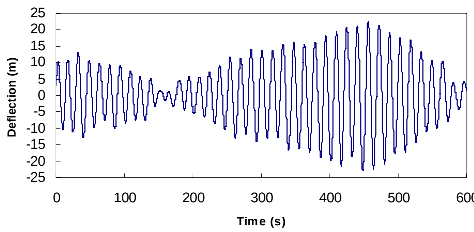

a) Vertical displacement, α_a = 0 degree

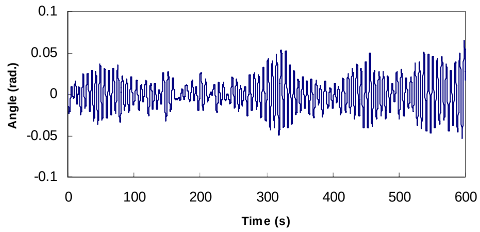

b) Torsion, α_a = 0 degree

Fig. 9 Responses of original section Akashi Kaikyo Bridge with buffeting force only (U = 60 m/s)

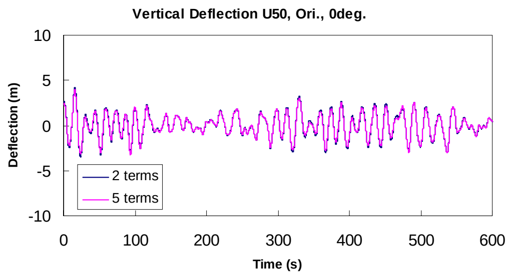

a) Vertical displacement, α_a = 0 degree, 2 and 5 lag terms

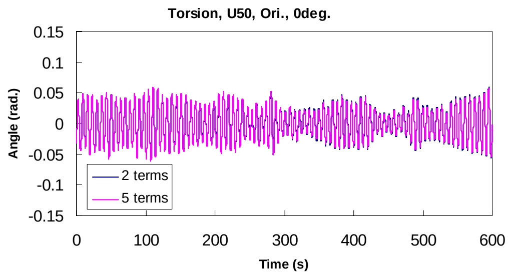

b) Torsion, α_a = 0 degree, 2 and 5 lag terms

Fig. 10 Responses of original section of Akashi Kaikyo Bridge with buffeting and self-excited forces (U = 50 m/s)

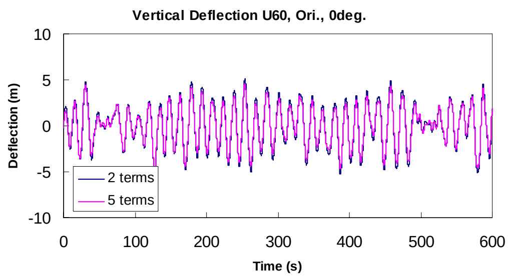

a) Vertical displacement, α_a = 0 degree, 2 and 5 lag terms

Fig. 11 Responses of original section of Akashi Kaikyo Bridge with buffeting and self-excited forces (U = 60 m/s)

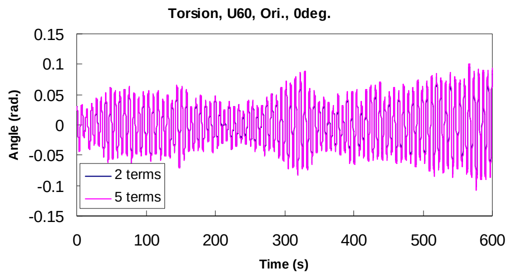

b) Torsion, $\alpha_a = 0$ degree, 2 and 5 lag terms

Fig. 11 Responses of original section of Akashi Kaikyo Bridge with buffeting and self-excited forces ($U = 60$ m/s) (cont.)

6. Effect of Evaluation Function

Another important issue in the rational function approximation technique is the effect of weighting factor w_{ij}. In this part, the approximation process with other evaluation functions $J = \sqrt{\sum_{i=1}^{2}\sum_{j=1}^{2} w_{ij}\varepsilon_{ij}}$, based on changing the weighting factor w_{ij} , will be carried out to define the effect of function J. Only tabular data of original section of 0 degree with 4 lag terms is used to analyze with three cases of J as follows:

Case 1: considering the total error with same factor w_{ij},

$$J_1 = \sum_{i=1}^{2}\sum_{j=1}^{2}\varepsilon_{ij}$$

Case 2: the factor w_{ij} will be selected depending on the magnitude of Q_{ij},

$$J_2 = \varepsilon_{11} + \varepsilon_{12} + 10\varepsilon_{21} + 100\varepsilon_{22}$$

Case 3: only considering the minimum error of Q_{22},

$$J_3 = \sum_{i=1}^{2}\sum_{j=1}^{2}\varepsilon_{22}$$

Fig. 12 shows the obtained approximation results in the three cases. Although the shape of approximated curve of Q_{22} in case 2 and case 3 is better than that in case 1, the total error in case 1 is much smaller than other cases as shown in Fig. 13. This is because the absolute errors of Q_{11}, Q_{12} and Q_{21} are larger and dominant in the total error. However, the structure's responses, both vertical deflection and torsion, are almost same in 3 cases as shown in Fig. 14. As similar to 5.2, the response is insensitive approximation error. This must be carefully examined if the approximation error does not affect the response or the approximate error at the wind speed analyzed happens to be small among the cases compared. That demonstrates the weighting factor doesn't have a significant role in wind-induced response with rational function approximation technique.

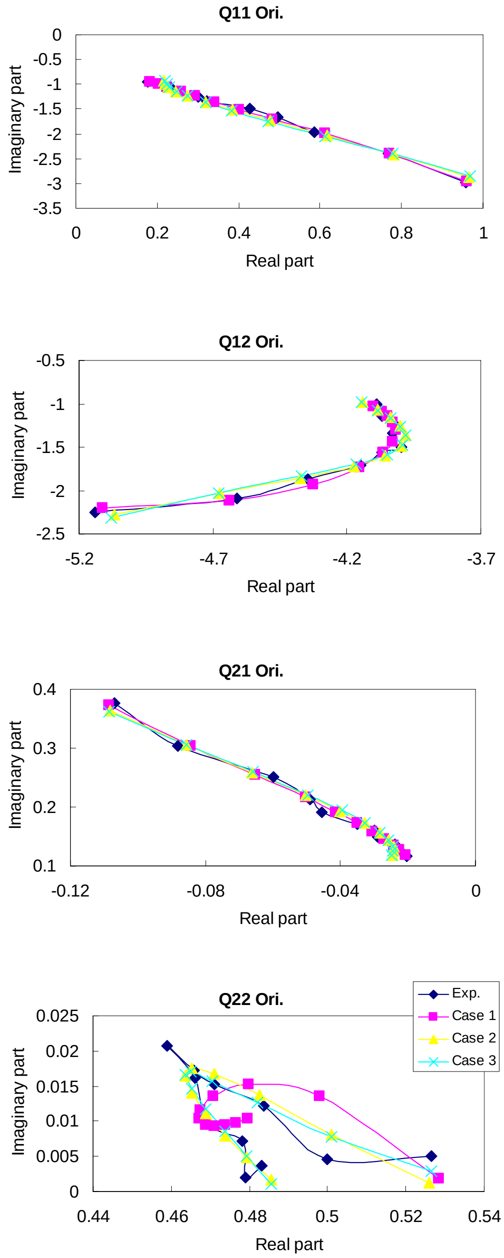

Fig. 12 Approximation results for original section, $\alpha_a = 0$ degree, 4 lag terms in three cases

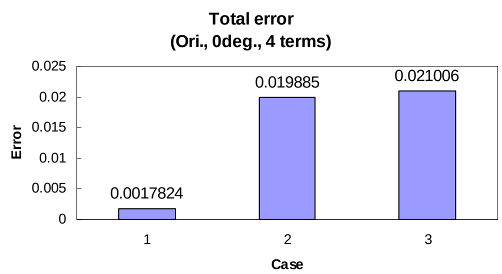

Fig. 13 Total error between approximation result and experiment result in three cases

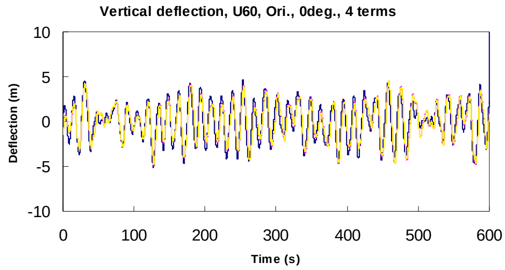

a) Vertical displacement

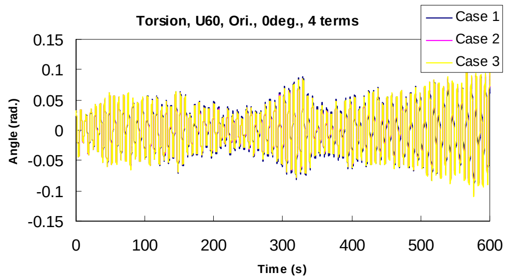

b) Torsion

Fig. 14 Approximation results of original section, α_a = 0 degree, 4 lag terms in three cases (U = 60 m/s)

7. Conclusion

Analytical investigations on rational function approximation technique for wind-induced response analysis of a long-span bridge in time domain were presented using the Akashi Kaikyo Bridge data. In particular, the sensitivity of the approximation to the response was focused on. Conclusions obtained are summarized as follows:

[1] Approximation can be succeeded even for real bridge flutter derivatives if using larger number of lag terms. The more lag terms were used, the smaller total error was obtained. Even in a real bridge case, at least 4 lag terms will be enough with respect to approximation error.

[2] Time-domain response analysis by the rational function approximation technique can well capture the transient response at near the critical wind speed.

[3] The total approximation error was not significant to the bridge response. However, this may be due to the fact that the approximation error at the wind speed analyzed happened to be small. Or significant difference may arise if the total approximation error becomes larger than the range in this study.

In future, this insignificance should be further examined, e.g., using flutter derivatives of other long-span bridges.

References

1) E. Simiu, R. H. Scanlan, *Wind Effects on Structures Fundamentals and Applications to Design*, Third Edition, John Wiley & Sons, Inc., New York,1996.
2) R.H. Scanlan, N. P. Jones, Aeroelastic analysis of cable-stayed bridge, *Journal of Structural Engineering*, ASCE, Vol. 116(2), 1990.
3) A. Jain, N. P. Jones and R. H. Scanlan, Couple flutter and buffeting analysis of long-span bridge, *Journal of Structural Engineering*, ASCE, Vol. 122(7), 1996.
4) V. Boonyapinyo, T. Miyata and H. Yamada, Advanced Aerodynamic Analysis of Suspension Bridges by State-space Approach, *Journal of Structural Engineering*, ASCE, Vol. 125(12), 1999.
5) X. Chen, M. Matsumoto and A. Kareem, Time Domain Flutter and Buffeting Response Analysis of Bridges, *Journal of Engineering Mechanics*, ASCE, Vol. 126(1), 2000.
6) K. Wilde, Y. Fujino and J. Masukawa, Time Domain Modeling of Bridge Deck Flutter, *Journal of Structural Mechanics and Earthquake Engineering*, JSCE, No. 543, 1996.
7) K. L. Roger, Airplane Math Modeling for Active Control Design, AGARD CP-228, 1977.
8) X. Chen and A. Kareem, Efficacy of the Implied Approximation in the Identification of Flutter Derivatives, *Journal of Structural Engineering*, ASCE, Vol. 130(12), 2004.

(Received September 18, 2007)